An Approach Toward the Synthesis of Platelike Ordered Mesoporous Materials from Layered Zeolite Precursors

Raquel García, Isabel Díaz, Carlos Márquez-Álvarez, and Joaquín Pérez-Pariente*

Instituto de Catálisis y Petroleoquímica, CSIC, C/Marie Curie 2, Cantoblanco, 28049-Madrid, Spain

Received December 26, 2005. Revised Manuscript Received February 20, 2006

An ordered silicate mesophase has been synthesized via a hydrothermal treatment of a lamellar cetyltrimethylammonium-intercalated complex. The precursor was obtained by reaction of the layered silicate Na−RUB-18 with the cationic surfactant cetyltrimethylammonium chloride at pH 11.5. Hydrothermal transformation of this lamellar phase into an MCM-41-type mesoporous silicate was studied by powder X-ray diffraction, thermogravimetric analysis, ^{29}Si magic-angle spinning NMR, Fourier transform infrared spectroscopy, scanning electron microscopy, and transmission electron microscopy. The as-prepared mesoporous product formed after 5 days of hydrothermal treatment retains the platelike morphology and most of the local ordering of the parent material. Removal of template by calcination drastically decreases the crystallinity, although lower temperature treatment with ozone partly preserved the crystalline structure. The final mesoporous material shows very thin platelike morphology, with MCM-41-type of channels perpendicular to the plates.

Introduction

The family of ordered mesoporous materials prepared under hydrothermal conditions from silicate/aluminosilicate gels containing surfactant molecules have attracted much attention in recent years due to their potential applications in several fields as catalysts, adsorbents, and catalysts carriers.[1] However, for certain catalytic applications, the typically amorphous nature of the walls (framework) in these mesoporous materials is a drawback. On the basis of what is known about zeolite chemistry, different synthesis strategies have been developed in order to improve framework ordering in mesoporous materials.[2] One of the attempts was to prepare mesoporous materials by reaction of the single-layered silicate kanemite with surfactant molecules.[3,4] The interest of employing such layered precursors in the synthesis of mesoporous solids lies in the thought that some of the structural characteristics of the parent material will remain on the mesoporous phase. Following this approach, mesoporous materials FSM-16 formed from the fragmentation of individual silicate sheets of kanemite were reported and widely studied.[5] These materials possess a hexagonal arrangement of unidirectional pore channels similar to that of the MCM-41 structure, but they show different thermal stability and adsorption properties, which is usually attributed to a higher condensation of the framework of the kanemite-derived mesoporous silicate.[6] However, the differences in the pore wall structures of the MCM-41 hexagonal phase and FSM-16 have not yet been clarified.[7]

The formation of a disordered mesoporous material (KSW-1)[8] and the formation of a mesoporous silica with rectangular arrangements of unidirectional channels (KSW-2)[9] upon changing the synthesis conditions in the reaction of kanemite with alkyltrimethylammonium surfactants have also been reported. The mechanism of formation of KSW-2 is thought to proceed via bending of the individual silicate sheets rather than by their fragmentation. This would explain the unique pore system of this material.[10]

Attempts to prepare mesoporous materials from layered precursors with a more complex structure of the layer have only been scarcely explored and they have always led to lamellar mesophases that collapsed upon calcination.[11,12] Multilayered silicates possess thicker tetrahedral layers with a significant amount of Q^4 silicate species that makes the silicate layer more rigid than those of single-layered silicates, preventing the bending or fragmentation of the sheets that is required to form the mesoporous material. However, many of these multilayered silicates have building units that are usually found in zeolites, and indeed, some of them yield zeolitic frameworks upon calcination, such as PREFER/ferrierite,[13] AMH-3,[14] and Nu-6(1)/Nu-6(2).[15] Thereby, they are ideal candidates to obtain mesoporous solids with improved properties. Among them, those with higher Q^3/Q^4 ratio would be more reactive, flexible, and therefore suitable for interaction with surfactant molecules. In this sense, a

* Corresponding author. Phone: + 34 91 5854784. E-mail: jperez@icp.csic.es.

(1) Corma, A. *Chem. Rev.* **1997**, *97*, 2373.
(2) Pérez-Pariente, J.; Díaz, I.; Agúndez, J. *C. R. Chimie* **2005**, *8*, 569.
(3) Yanagisawa, T.; Shimizu, T.; Kuroda, K.; Kato, C. *Bull. Chem. Soc. Jpn.* **1990**, *63*, 988.
(4) Inagaki, S.; Fukushima, Y.; Kuroda, K. *J. Chem. Soc. Chem. Commun.* **1993**, 680.
(5) Chen, C.-Y.; Xiao, S. Q.; Davis, M. E. *Micropor. Mater.* **1995**, *4*, 1.
(6) Matsumoto, A.; Sasaki, T.; Nishimiya, N.; Tsutsumi, K. *Colloids Surf. A* **2002**, *203*, 185.
(7) Inagaki, S.; Sakamoto, Y.; Fukushima, Y.; Terasaki, O. *Chem. Mater.* **1996**, *8*, 2089.
(8) Ryoo, R.; Kim, J. M.; Ko, C. H.; Shin, C. H. *J. Phys. Chem.* **1996**, *100*, 17718.
(9) Kimura, T.; Kamata, T.; Fuziwara, M.; Takano, Y.; Kaneda, M.; Sakamoto, Y.; Terasaki, O.; Sugahara, Y.; Kuroda, K. *Angew. Chem., Int. Ed.* **2000**, *39*, 3855.
(10) Shigeno, T.; Inoue, K.; Kimura, T.; Katada, N.; Niwa, M.; Kuroda, K. *J. Mater. Chem.* **2003**, *13*, 883.
(11) Sprung, R.; Davis, M. E.; Kauffman, J. S.; Dybowsky, C. *Ind. Eng. Chem. Res.* **1990**, *29*, 213.
(12) Song, M. G.; Kim, J. D.; Kiyozumi, Y. *Stud. Surf. Sci. Catal.* **2003**, *146*, 169.

10.1021/cm052855m CCC: $33.50
Published on Web 03/31/2006

Table 1. Synthesis Conditions and Textural Properties of the Different Materials Derived from Na−RUB-18

	as-made						
	synthesis conditions					calcined textural properties	
sample	$CTA/SiO_2/H_2O$	pH_i[a]	T[b] (°C)	time[c] (h)	product	S_{BET}[d] (m^2/g)	Pd[e] (nm)
Na−RUB-18	−	−	−	−	−	17	−
R1	0.18/1/98	8.1	nontreated		swollen	12	−
R2a	0.18/1/98	11.5	80	3	swollen	−	−
R2b	0.18/1/98	11.5	80	24	swollen	28	−
R3a	0.18/1/98	11.5	nontreated		swollen + RUB-18	16	−
R3b	0.18/1/98		150	3	swollen + mesostructured	111	2.5
R3c	0.18/1/98		150	120	mesostructured	242	2.7
						195[f]	2.8[f]
R3d	0.18/1/98		150	408	mixture with silicalite-1	−	−
R4a	0.09/1/95	11.5	nontreated		swollen + RUB-18	−	−
R4b	0.09/1/95	11.5	150	24	swollen	−	−
R4c	0.09/1/95	11.5	150	36	swollen + mesostructured	252	2.7
R4d	0.09/1/95	11.5	150	48	swollen + mesostructured	212	2.8

[a] pH of the initial surfactant suspension. [b] Temperature of the hydrothermal treatment. [c] Time duration of the hydrothermal treatment. [d] Specific surface area calculated following the BET procedure. [e] Pore diameter determined following the BJH method on the adsorption branch. [f] Sample treated at lower temperature with ozone in oxygen.

promising prospect is the synthetic layer silicate RUB-18,[16] which is isostructural to the layered silicates octosilicate and ilerite.[17] The basic building unit of the RUB-18 sheet is the [5^4] cage, consisting of four five-membered rings. This is a building unit found in zeolite structures such as MFI and MOR. In RUB-18, four silicon atoms of each cage are connected to four neighboring cages via eight oxygen bridges forming the sheet.[16] These layers are separated from each other by chains of edge-sharing $[Na(H_2O)_6]^+$ octahedra that compensate for the negative charge of the layers. This confers the silicate RUB-18 cationic exchange properties. Furthermore, the topotactic condensation of the intercalated layer material RUB-18 into a new zeolite (RUB-24) with RWR structure has been recently reported.[18]

In this work, we report a novel method to prepare a mesoporous material through the reaction of the complex layer silicate precursor RUB-18 with the cationic surfactant cetyltrimethylammonium chloride followed by a hydrothermal treatment. Flat and thin crystals with mesoporous channels in the direction perpendicular to the plate plane are obtained. Several techniques, such as ^{29}Si MAS NMR, FTIR, and TEM have been used to follow the transformation from a zeolite-type of structure to a mesoporous MCM-41-type of material. The successful synthesis of a mesoporous solid from this precursor opens up a field for further development on the search of mesoporous materials with highly ordered frameworks.

Experimental Section

Preparation of Starting Material, Na−RUB-18. The synthesis of the parent layered silicate has been carried out as follows. Sodium hydroxide (0.94 g) was dissolved in water (183.8 g) at 50 °C. To this solution, 15 g of hexamethylenetetraamine (Aldrich, 99%) and 40 g of sodium trisilicate hydrate ($Na_2Si_3O{\cdot}H_2O$, Aldrich) were finally added. After 1 h of stirring, the gel was loaded in 50-mL Teflon-lined autoclaves and heated statically at 100 °C for 1 month. The solid product was recovered by filtration, thoroughly washed with water and ethanol, and dried at room temperature.

Preparation of the Surfactant−RUB-18 Mesophases and Thermal Treatment. The surfactant−RUB-18 materials were prepared by heating a suspension of Na−RUB-18 in an aqueous solution containing cetyltrimethylammonium (CTA) cations (Na−RUB-18/surfactant solution ratio of 1 g/20 mL) at 80 °C for 3 h. The pH and composition of the suspensions were varied as stated in Table 1 by using mixtures of cetyltrimethylammonium hydroxide and chloride. The surfactant solutions were prepared using a commercial CTACl aqueous solution (Fluka, 25 wt %) and deionized water. An anion-exchange resin was used to obtain the hydroxide solutions. After this treatment, the suspensions were placed in Teflon-lined stainless steel autoclaves and heated statically at different temperatures in the range from 80 to 150 °C. The products were recovered by filtration, washed with water and ethanol, and dried at room temperature.

In a representative preparation, 1.14 g of Na−RUB-18 was mixed with 20 mL of 0.1 M CTACl solution and 3 mL of CTAOH solution (ca. 0.1 M). The pH of the initial mixtures was typically 11.5−11.7. After refluxing at 80 °C for 3 h (typical final pH 10.2−10.4), the suspension was loaded in 30-mL Teflon-lined stainless steel autoclaves and heated at 150 °C for 5 days.

Surfactant Removal. The samples were calcined at 450 °C under continuous flow of N_2 (100 mL/min) for 1 h followed by air (100 mL/min) for 6 h in order to obtain the mesoporous material free from surfactant. Selected samples were calcined in N_2 (70 mL/min) at 260 °C for 1 h, followed by treatment with a flow of ozone/oxygen (60 mL/min, ca. 2 vol % O_3) at 200 °C for 72 h. Ozone in oxygen stream was produced using an ECO-5 ozone generator manufactured by SALVECO Proyectos, S. L. Thermogravimetric analysis of the samples was carried out to ensure that the residual amount of organic in the samples was less than 5 wt % after these treatments.

Characterization. Powder X-ray diffraction (XRD) patterns were obtained with a Seifert XRD 3000P diffractometer using monochromatic Cu Kα radiation. Thermogravimetric analysis (TGA) was carried out using a Perkin-Elmer TGA7 instrument at a heating rate of 20 °C/min under air flow. The organic fractions were

(13) Schreyeck, L.; Caullet, P.; Mougenel, J. C.; Guth, J. L.; Marler, B. *Micropor. Mater.* **1996**, *6*, 259.
(14) Jeong, H. K.; Nair, S.; Vogt, T.; Dickinson, D.; Tsapatsis, M. *Nat. Mater.* **2003**, *2*, 53.
(15) Zanardi, S.; Alberti, A.; Cruciani, G.; Corma, A.; Fornes, V.; Brunelli, M. *Angew. Chem., Int. Ed.* **2004**, *43*, 4933.
(16) Vortmann, S.; Rius, J.; Siegmann, S.; Gies, H., *J. Phys. Chem. B* **1997**, *101*, 1292.
(17) Brenn, U.; Ernst, H.; Freude, D.; Herrmann, R.; Jähnig, R. J.; Karge, H. G.; Kärger, J.; König, T.; Mädler, B.; Pingel, U. T.; Prochnow, D.; Schwieger, W. *Micropor. Mesopor. Mater.* **2000**, *40*, 43.
(18) Marler, B.; Ströter, N.; Gies, H. *Micropor. Mesopor. Mater.* **2005**, *83*, 201.

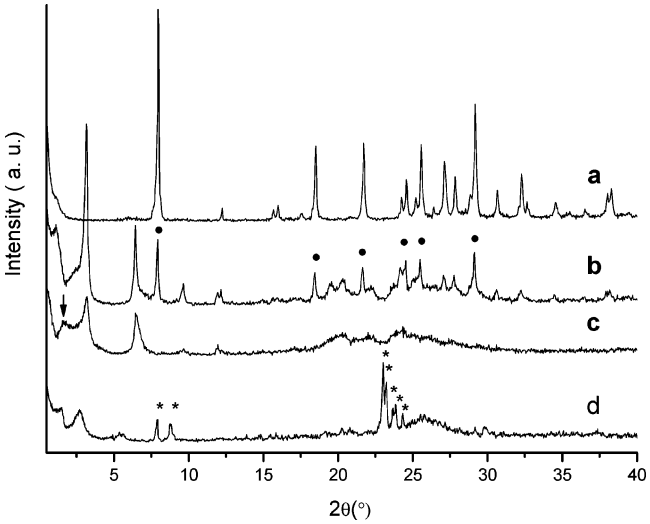

Figure 1. XRD patterns of (a) as-prepared Na−RUB-18; (b) swollen material R3a containing residual Na−RUB-18 phase (diffractions indicated with black dots); (c) sample R3c, the former material further hydrothermally treated at 150 °C for 5 days (black arrow shows the developed low angle diffraction); (d) sample R3d, material hydrothermally treated for 17 days (asterisks indicate diffractions of silicalite-1).

quantified by C, H, N analysis using a Perkin-Elmer 2400 CHN analyzer. FTIR spectra using the KBr pellet technique (ca. 0.5 mg of sample in 250 mg of KBr) were collected with a Nicolet 5ZDX FTIR spectrometer provided with an MCT detector. The spectra were obtained by averaging 256 scans in the 400−4000 cm^{-1} wavenumber range, at 4 cm^{-1} resolution, and using Happ−Genzel apodization. The MAS NMR spectra were recorded with a Bruker AV 400 spectrometer using a BL7 probe for ^{29}Si and ^{13}C. The samples were spun at 5−5.5 kHz at the magic angle. ^{29}Si spectra were acquired using pulses of 3.3 μs (to flip the magnetization $3\pi/8$ rad) and a recycle delay of 240 s. ^{13}C cross polarization (CP) spectra were recorded using $\pi/2$ rad pulses of 4.5 μs and a recycle delay of 3 s. Nitrogen adsorption−desorption isotherms were measured at 77 K using a Micromeritics TRISTAR 3000 volumetric apparatus. Specific surface areas were calculated following the BET procedure. Pore diameter has been estimated by applying the BJH method to the adsorption branch of the isotherm. SEM micrographs were obtained using a JEOL JSM 6400 Phillips XL30 microscope operating at 20 kV. Transmission electron microscopy (TEM) coupled with selected area electron diffraction (SAED) studies were carried out in a JEOL-2000FX microscope, SAED patterns were recorded at a camera length of 60 cm in all cases. High-resolution (HRTEM) images were taken with a JEOL-4000 EX microscope operating at 400 kV (Cs = 1.0 mm).

Results

The powder X-ray diffraction pattern of the parent material (Figure 1a) agrees well with the XRD pattern reported in the literature for Na−RUB-18.[16] All the reflections are characteristic of RUB-18 and indicate that the product is highly crystalline and free from impurities.

The initial refluxing of Na−RUB-18 with the surfactant solution at 80 °C and pH 11.5 resulted in the swelling of the original phase, as revealed by the XRD results (Figure 1b). The pattern of this product exhibits three diffraction peaks at $2\theta = 3.18$, 6.45, and 9.63°, corresponding to d spacings of 2.78, 1.37, and 0.92 nm, respectively (note that the broad peak at low angle in this diffractogram is an artifact). These values follow the correlation d, $d/2$, $d/3$, allowing identification of a lamellar structure due to the intercalation of the cetyltrimethylammonium molecules between the layers of RUB-18, in agreement with the results reported previously for a CTA−octosilicate complex.[19] However, the presence of reflections in the XRD pattern corresponding to Na−RUB-18 (marked with dots in Figure 1b) indicates that not all the interlayer spacings were expanded. After a subsequent hydrothermal treatment at 150 °C for 5 days, no reflections corresponding to the Na−RUB-18 phase appear in the XRD pattern (Figure 1c), indicating that this treatment allowed complete swelling of the layered material. Furthermore, the diffractions corresponding to the swollen CTA−RUB-18 phase became less intense and a new broad diffraction peak appeared at a low angle $2\theta = 1.56°$ (marked with an arrow in Figure 1c), corresponding to a large d spacing (5.65 nm). This result suggests that a new mesophase is obtained at the expenses of the lamellar CTA−RUB-18 complex formed after the initial refluxing. Assuming that this reflection corresponds to the d_{100} spacing in an MCM-41-type hexagonal arrangement of pores (*p6mm* symmetry), the unit cell parameter would be 6.5 nm according to the equation $a_0 = 2d_{100}/\sqrt{3}$. Extensive hydrothermal treatment at 150 °C for a prolonged period of time (up to 17 days) led to an XRD pattern (Figure 1d) where the peaks characteristic of the crystalline microporous zeolite silicalite-1 can be identified, together with broader and less intense reflections of a lamellar product. Crystallization of silicalite-1 (MFI) is probably due to the decomposition of the surfactant molecules in smaller fragments as previously proposed by Huang et al.[20]

Incorporation of the surfactant within the RUB-18 silicate layers was followed by thermal analysis. Table 2 and Figure 2 illustrate representative TGA data for the original layered Na−RUB-18, as well as the CTA−RUB-18 complex and the sample hydrothermally treated at 150 °C for 5 days (samples R3a and R3c, respectively). The Na−RUB-18 sample shows only a main weight loss step of about 15 wt % below 130 °C, due to the desorption of water occluded between the layers, as typically found for a layered compound crystallized in the absence of organic template. After the refluxing and the hydrothermal treatments in the presence of CTA, the samples show an additional weight loss between 130 and 600 °C due to the decomposition and removal of the CTA species. From the TGA data, the amount of surfactant in these samples was estimated to be in the range 35−40 wt %, which is close to the typical surfactant content in as-made MCM-41 silica samples. Moreover, the organic content of the samples, determined by C, H, N analysis (Table 2), agrees well with the amount of surfactant given by thermogravimetric analysis, and the C/N ratio close to the theoretical value (C/N = 19) indicates that the surfactant molecules are intact within the solids. This is supported by ^{13}C MAS NMR spectra of the hydrothermally treated samples (not shown).

The absence of Bragg reflections in the XRD patterns of calcined samples Na−RUB-18 and swollen CTA−RUB-18 composite indicates the collapse of the structure upon this

(19) Endo, K.; Sugahara, Y.; Kuroda, K. *Bull. Chem. Soc. Jpn.* **1994**, *67*, 3352.
(20) Huang, L.; Chen, X.; Li, Q. *J. Mater. Chem.* **2001**, *11*, 610.

Table 2. Thermogravimetric and Chemical Analyses of the Original Na−RUB-18, As-Made Swollen Sample R3a, and As-Made Hydrothermally Treated Sample R3c

	TG analyses (wt %)		chemical analyses				
sample	step I: 35 °C < *T* < 130 °C	step II: 130 °C < *T* < 600 °C	C (wt %)	N (wt %)	H (wt %)	C/N	CTA[a] (wt %)
Na−RUB-1 8	14.7	–	–	–	–	–	–
R3a	5.7	40.1	30.0	1.9	6.4	18.4	38.7
R3c	3.4	34.1	26.6	1.7	5.5	18.3	34.6

[a] Theoretical value calculated from the nitrogen content (chemical analysis) and assuming C/N = 19.

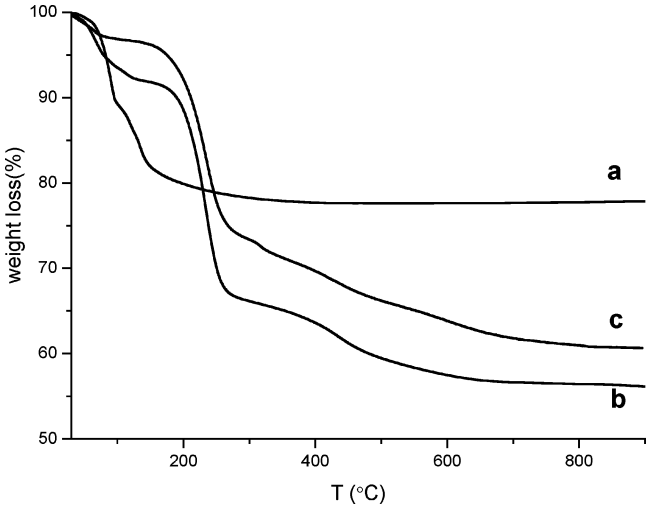

Figure 2. Thermogravimetric analysis of (a) Na−RUB-18; (b) swollen material, sample R3a; (c) material further hydrothermally treated for 5 days at 150 °C, sample R3c.

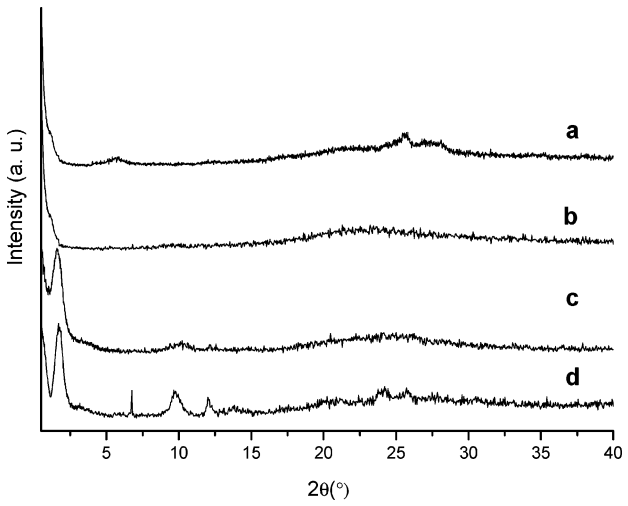

Figure 3. XRD diffraction patterns of samples calcined in air: (a) Na−RUB-18, (b) swollen sample R3a, (c) sample R3c, and (d) sample R3c treated with ozone in oxygen stream.

thermal treatment (Figure 3a,b). In contrast, the XRD pattern of sample R3c calcined (Figure 3c) retains the low-angle reflection at ca. $2\theta = 1.62°$ ($d = 5.45$ nm), indicating that the mesoporous structure is stable to calcination with little shrinkage of the framework. The XRD pattern of the sample obtained when the surfactant was removed at low temperature using ozone (Figure 3d) shows the low angle diffraction corresponding to a unit cell parameter (a_0) of 6.3 nm, and two additional broad diffractions at high angle $2\theta = 9.75°$ ($d = 0.91$ nm) and $2\theta = 12.08°$ ($d = 0.73$ nm); note that the sharp reflection at 7° is a spurious peak. Thus, it is possible that such a mild treatment helps to keep some atomic

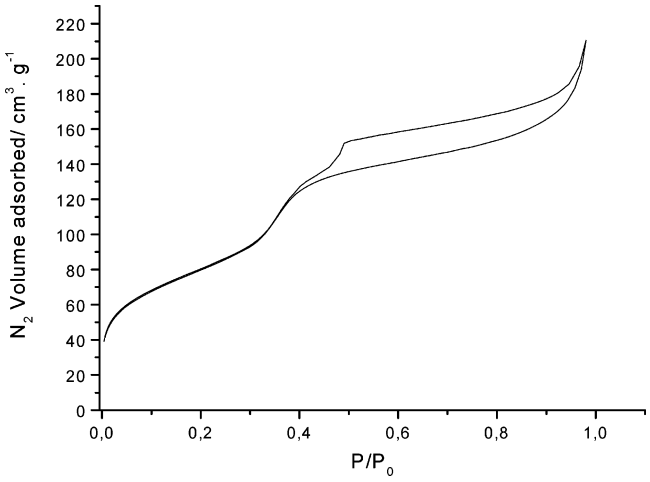

Figure 4. N_2 adsoption−desorption isotherm of sample R3c after calcination.

order of the parent silicate precursor, besides the mesoporous structure.

BET surface area and pore size of selected calcined samples are given in Table 1. As expected, the original Na−RUB-18 phase and swollen samples show a small surface area due to the collapse of the structure upon calcination. On the other hand, the samples hydrothermally treated for 5 days at 150 °C calcined in air showed a type IV nitrogen adsorption isotherm (Figure 4) characteristic of a mesoporous material with narrow pore size distribution. It is worth mentioning that the calcined sample heated at 80 °C for 24 h does not show this type of isotherm while the sample treated at 150 °C for 3 h shows mesoporosity. Furthermore, extending the heating to 5 days results in a BET surface area of 242 m^2/g, pore volume of 0.28 cm^3/g, and pore size of 2.7 nm. Slightly lower BET surface area (195 m^2/g) and pore volume (0.26 cm^3/g) are obtained for the same material when the surfactant was removed by ozone treatment. Although the isotherms show a very narrow pore size distribution within the pore size diameter commonly obtained for MCM-41, the S_{BET} and pore volume values are low compared to those of conventional mesoporous materials.[21] An exhaustive analysis of the material by electron diffraction allows us to discard an eventually significant contribution of amorphous phase. Therefore, these low textural values could be due to a very thick pore wall (ca. 4 nm) estimated as the difference between the unit cell parameter (6.3 nm) and the pore diameter (2.7 nm).

Electron Microscopy Results. Scanning electron microscopy (SEM) and transmission electron microscopy (TEM)

(21) Sen, T.; Tiddy, G. J. T.; Casci, J. L.; Anderson, M. W. *Angew. Chem., Int. Ed.* **2003**, *42*, 4649.

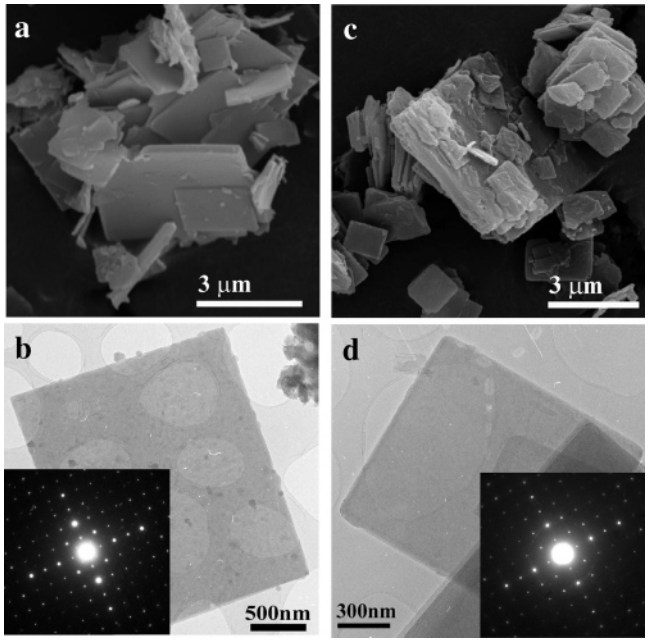

Figure 5. Electron microscopy results of Na−RUB-18 (a, b) and swollen sample R3a (c, d): (a and c) SEM micrographs and (b and d) low-magnification TEM images and corresponding SAED patterns.

have been used in order to study the transformation from the layered silicate Na−RUB-18 to a swollen layered silicate and further to an ordered layered mesoporous material. In general terms, SEM provides the morphology information and TEM allows identification of the internal structure within the layered crystals. More specifically, selected area electron diffraction (SAED) patterns coupled with high-resolution transmission electron microscopy (HRTEM) images constitute a powerful tool to analyze the evolution of the crystalline structure forming the layers toward the final mesoporous material. Unfortunately, the lack of stability of some zeolite-type of structures under the electron beam, leading to crystal structure vanishing and cation migration during the observations, is well-known; Na−RUB-18 is of those cases. However, some relevant information has been extracted from these studies, as reported below.

Figure 5 collects SEM (Figure 5a) and TEM (Figure 5b) images of the original Na−RUB-18 crystals, showing the typical morphology of thin tetragonal platelets, along with the SAED pattern corresponding to a highly crystalline material.[16] It is worth noting that the analysis of the obtained SAED patterns and a deep study of electron diffraction tilting series suggest a lowering in the symmetry from the tetragonal *I*41/*amd* space group that has been assigned to the RUB-18 structure.[16] This is probably due to the migration of the Na cations during the observations, as the crystalline structure of this material has been confirmed by the XRD data shown above. The initial refluxing with the surfactant solution did not substantially alter the platelike morphology of the crystals (Figure 5c). Furthermore, TEM/SAED analysis (Figure 5d) corroborates that both crystal shape and atomic structure of the RUB-18 layers are not modified by the surfactant intercalation treatment.

SEM micrographs collected in Figure 6 show some of the products obtained using diverse CTA concentration and hydrothermal treatment conditions to illustrate the optimization of the sample preparation parameters. The use of a low surfactant/Si ratio (0.09) led to apparent crystal dissolution during the hydrothermal treatment at 150 °C in a period of time as short as 2 days (Figure 6a). Increasing the surfactant/Si ratio to 0.18 resulted in notably less damaged crystals, which retained the morphology of the parent RUB-18 silicate, even after a more severe hydrothermal treatment at 150 °C for 5 days (Figure 6b). However, a prolonged hydrothermal treatment for 17 days gave rise to the growth of big twinned crystals with the characteristic shape of silicalite-1 zeolite (Figure 6c), which were previously identified by XRD.

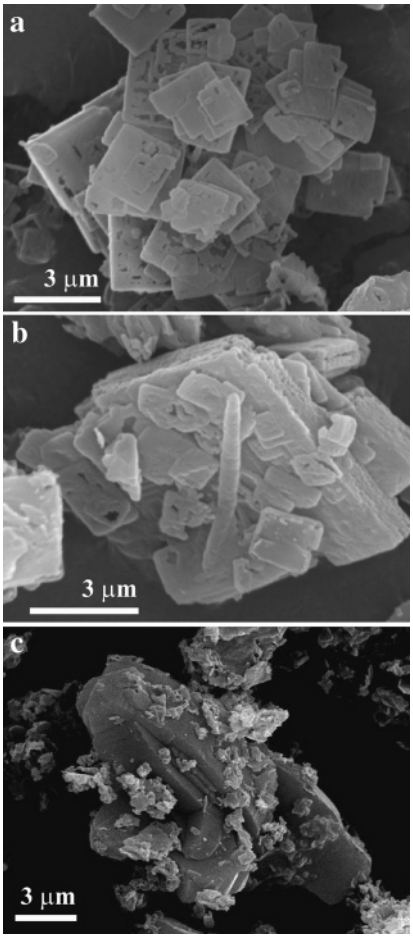

Figure 6. Scanning electron micrographs of (a) sample R4d, material synthesized with a Si/surfactant ratio of 0.09 and hydrothermally treated at 150 °C for 2 days; (b) sample R3c, material hydrothermally treated at 150 °C for 5 days; (c) sample R3d, material synthesized with a Si/surfactant ratio of 0.18 and hydrothermally treated at 150 °C for 17 days.

Further TEM studies, shown in Figure 7, demonstrate that the crystal structure of the layers has drastically changed after 5 days of hydrothermal treatment at 150 °C and that a mesoporous structure develops all over the inner area of the platelike crystals in as-made sample R3c. Figure 7a shows a typical low-magnification image of this sample and its corresponding SAED pattern. Interestingly, both the morphology and the electron diffraction pattern resemble those of the parent RUB-18 structure but with evidenced lowering in the crystallinity. A careful analysis and processing of the images shows that this remaining atomic symmetry may be due to residual RUB-18 that has not been transformed into mesoporous phase. The shape of the crystals remains tetragonal platelike but noticeably thinner and with a thin

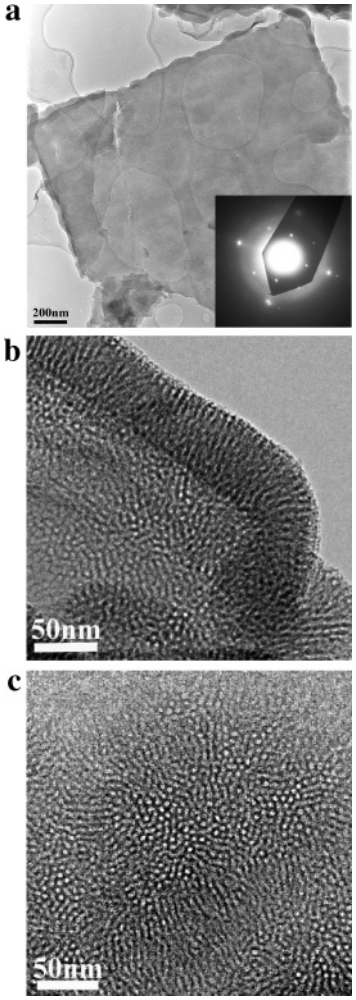

Figure 7. HRTEM results of sample R3c hydrothermally treated at 150 °C for 5 days, prior calcination: (a) low-magnification image and corresponding SAED pattern; (b and c) high-magnification images showing the edge and internal structures, respectively, of the mesoporous plates.

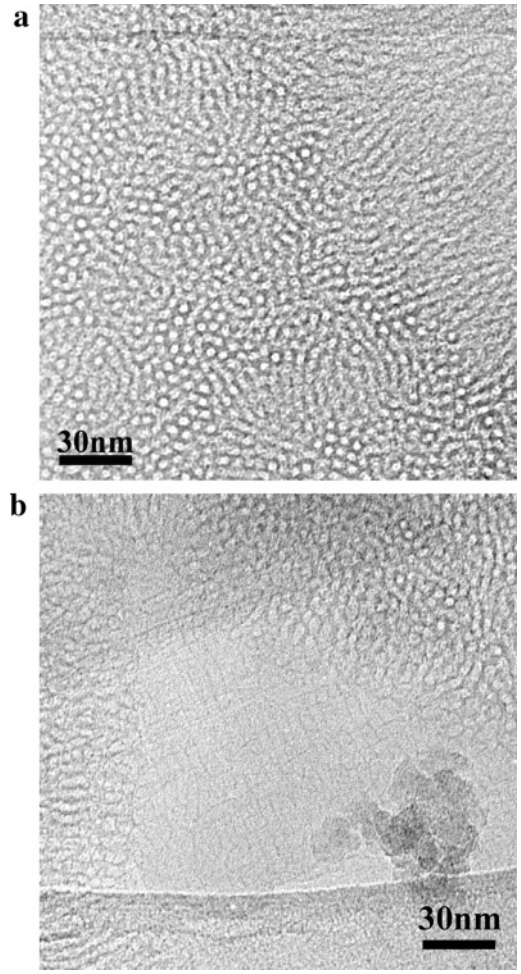

Figure 8. High-resolution TEM images of inner areas of sample R3c calcined.

mesoporous lamellar structure in the edges of the particles (Figure 7b), probably due to local dissolution and recrystallization of silica species. Indeed, silica yields after the refluxing and hydrothermal treatment at pH 11.5 and 150 °C for 5 days are 95% and 79%, respectively, indicating a certain degree of dissolution during the process. Figure 7c shows a representative TEM image of the bulk of the crystals that appear to be formed by ordered mesopores with a well-defined pore size and, more interestingly, with the pore mouth aligned perpendicular to the plate plane.

The tetragonal flat morphology, outer lamellar structure, and inner ordered mesoporous structure of as-made sample R3c remains unaltered after calcination in air at 450 °C, although TEM/SAED studies confirmed the absence of crystallinity in this case. High-magnification TEM images collected in Figure 8 show the mesostructure forming the continuous inner area of the crystals in sample R3c calcined in air, with the pore openings perpendicular to the plate plane. In Figure 8a it is possible to identify some hexagonal arrangements, with a roughly estimated unit cell parameter of ca. 6 nm, in good agreement with the a_0 value obtained by X-ray diffraction. Along with such a MCM-41 type of structure with short channels, there are some lower contrast areas (shown in Figure 8b) where an interesting phase transformation may be observed. A squarelike structure is observed in this image that seems to be an intermediate step of the solid-state transformation from the parent silicate crystalline structure to the ordered mesoporous silicate.

Treatment of the as-made sample R3c with ozone at moderate temperature leads to a more crystalline material, as evidenced by the exhaustive TEM/SAED analyses. Figure 9a shows a low-magnification image of a well formed tetragonal crystal and its corresponding SAED pattern. The analysis of the obtained SAED suggests a lowering in the crystallinity from the original RUB-18; however, in this case it was possible to obtain high-resolution images (Figure 9b) showing contrast with atomic ordering. Unfortunately, only fringes could be recorded due to the weakness of the sample under the electron beam. This crystalline atomic structure found in the inner areas of the crystals, next to a well-formed ordered mesoporous structure, corroborates the hypothesis of residual RUB-18 structure that has not been transformed. Finally, Figure 9c evidences the mentioned well-defined mesoporous structure present in the inner part of the crystals, with pore openings perpendicular to the plates.

FTIR and NMR Spectroscopies Characterization. Figure 10 shows the FTIR spectra of Na−RUB-18, swollen CTA−RUB-18 complex (sample R3a), hydrothermally treated material (sample R3c), sample R3c treated with ozone, and sample R3c calcined in air. The spectrum of the parent Na−

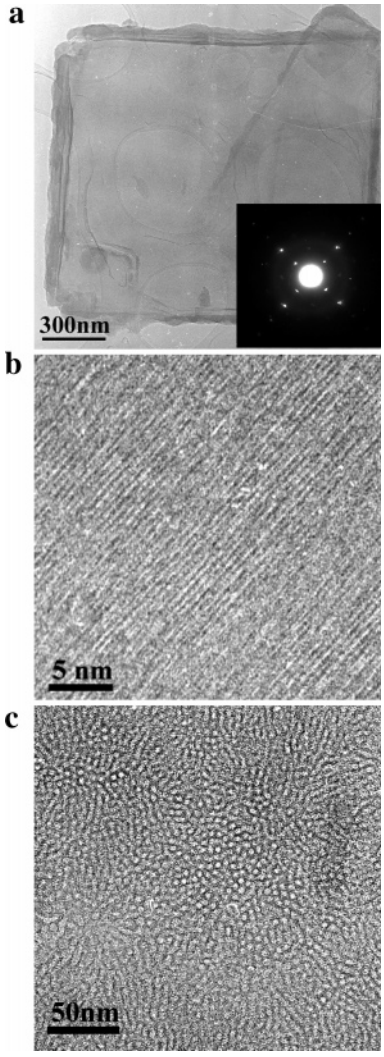

Figure 9. HRTEM results of sample R3c treated with ozone in oxygen stream. (a) Low-magnification image and corresponding SAED pattern. A series of higher resolution images at different focus allows identifying, in the inner part of the crystal, (b) fringes with atomic spacing and (c) mesoporous structure.

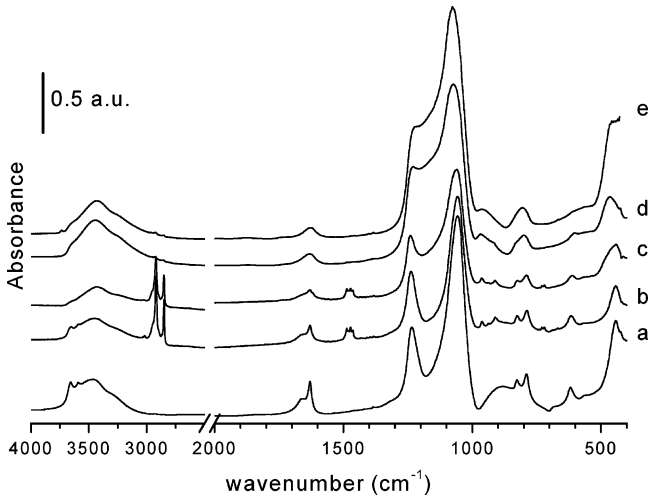

Figure 10. FTIR spectra of (a) Na−RUB-18, (b) swollen material, sample R3a; (c) material further hydrothermally treated for 5 days, sample R3c; (d) sample R3c treated with ozone in oxygen stream; and (e) sample R3c calcined in air.

RUB-18 closely matches the one previously reported for the layered silicate ilerite[22] and sodium octosilicate.[19] In the region of framework vibration modes, the spectrum is dominated by two strong and well-resolved bands at 1234 and 1057 cm^{-1} that can be assigned to the antisymmetric Si−O−Si stretching and the Si−O stretching of terminal Si−O^-/Si−OH groups, respectively. Furthermore, several bands of medium and weak intensity appear in the region of Si−O−Si symmetric stretching modes, at 826, 789, 618, and 443 cm^{-1}. These framework vibration bands are very narrow, a common feature in crystalline silicates and zeolites. In the spectrum of Na−RUB-18 there is also a broad band in this region (at ca. 880 cm^{-1}) that has been previously attributed to symmetric Si−O−Si stretching.[22] However, this band might correspond to Si−O−H deformation, as will be discussed later. Similarly to other layered silicates, the H−O−H bending of water molecules appears in the spectrum of Na−RUB-18 as a characteristic doublet, with maxima at 1660 and 1630 cm^{-1}. This splitting and the small bandwith seem to be characteristic of the water molecules octahedrally coordinating the interlayer sodium cations. Such water molecules would probably also give rise to the narrow O−H stretching bands at ca. 3590 and 3655 cm^{-1}.

The spectrum of the swollen sample (Figure 10, spectrum b) assesses the incorporation of surfactant molecules within the silicate. Characteristic methyl and methylene stretching and bending bands are observed in the regions 2850−3000 and 1400−1500 cm^{-1}, respectively, as well as methylene rocking at ca. 720 cm^{-1} and methyl rocking bands at 963 and 911 cm^{-1}. Concomitantly to the insertion of cetyltrimethylammonium species, the intensity of the narrow bands in the region of O−H bending and stretching attributed to water molecules linked to sodium cations decrease. This result suggests that the hydrated sodium cations of Na−RUB-18 were partially exchanged by CTA^+ ions during the refluxing treatment. The intercalation of surfactant molecules leads to partial removal of the broad band at 880 cm^{-1}, while all the narrow framework vibration bands that can be considered characteristic of the crystalline structure of the silicate layer are present in the spectrum of the swollen sample. This result suggests that the cation exchange does not produce a degradation of the crystalline structure and tends to discredit the assignment of the broad band at 880 cm^{-1} to a Si−O−Si stretching mode. We rather assign this band tentatively to Si−O−H deformation of silanol groups interacting by hydrogen bonding with water molecules of the $[Na(H_2O)_6]^+$ octahedra.

After hydrothermal treatment for 5 days (Figure 10, spectrum c) only a slight broadening of the framework vibration bands is observed, which indicates that the crystallinity of the sample is not significantly altered. Furthermore, there is no evidence of the formation of a noticeable amount of amorphous silicate. Only the development of a weak shoulder at ca. 465 cm^{-1} could be taken as an indication of the presence of amorphous material. The spectrum of sample R3c also shows that the surfactant is retained. On the other hand, sodium cations seem to be nearly quantitatively removed, as indicated by the disappearance of the corresponding OH stretching and bending bands, the later ones

(22) Huang, Y.; Jiang, Z.; Schwieger, W. *Chem. Mater.* **1999**, *11*, 1210.

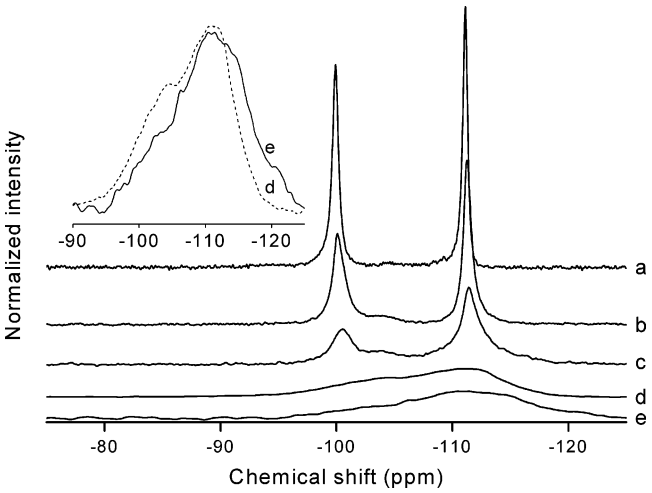

Figure 11. Solid-state ^{29}Si MAS NMR spectra of (a) Na−RUB-18; (b) swollen material, sample R3a; (c) material further hydrothermally treated for 5 days, sample R3c; (d) sample R3c treated with ozone in oxygen stream; and (e) sample R3c calcined in air. Spectra have been normalized to constant peak area sum.

being replaced by a broad and asymmetric band at ca. 1630 cm^{-1}, typical of adsorbed water molecules.

Treatment of sample R3c with ozone at as low a temperature as 200 °C quantitatively removes the surfactant, as evidenced by the absence of organic bands in the infrared spectrum (Figure 10, spectrum d). This treatment, however, has a marked effect on the framework vibration bands. A significant broadening of the band at ca. 1060 cm^{-1} occurs, together with an increase of the absorption in the region around 1150−1200 cm^{-1}. Furthermore, broad bands appear with maxima at ca. 968 and 465 cm^{-1}, and the resolution of the doublet around 800 cm^{-1} is highly reduced. All these features are a clear indication of the formation of amorphous silicate following the ozone treatment. Nonetheless, the band at 610 cm^{-1} is present, though with lower intensity than in the spectrum of sample R3c, and also the bands at 443 and 824 cm^{-1} can still be seen as shoulders. Therefore, the infrared data suggest that, although removal of the surfactant by the low-temperature ozone treatment leads to a major loss of crystallinity, some of the local ordering of the original sample is preserved.

Infrared data show that complete removal of the surfactant is also achieved by calcination in air at 450 °C (Figure 10, spectrum e). However, in contrast with the results described above, the infrared spectrum of sample R3c calcined in air is typical of amorphous silica and does not show any band characteristic of zeolitic-like structures. It can be concluded that the high temperature needed to remove the surfactant using air as the oxidizer causes a complete amorphization of the silicate.

Solid-state ^{29}Si MAS NMR spectra of representative samples are compared in Figure 11. The ^{29}Si MAS NMR spectrum of the parent Na−RUB-18 sample shows two sharp resonances at −99.9 and −111 ppm, with an intensity ratio of 51:49, which can be assigned to $Si(OSi)_3OH/Si(OSi)_3O^-$ (Q^3) and $Si(OSi)_4$ (Q^4) silicate species, respectively. Both chemical shift and intensity ratio are in close agreement with spectra reported for sodium octosilicate[19] and Na−RUB-18.[23] The spectrum of sample R3a, corresponding to the CTA−RUB-18 complex formed at pH 11.5, indicates that the crystalline structure of the silicate layers of Na−RUB-18 is mostly preserved after the surfactant intercalation. Only small changes in the spectrum are observed with respect to the parent material. The two narrow resonances due to Q^3 and Q^4 silicon species are observed at slightly higher field (−100.2 and −111.3 ppm, respectively). A small broadening of the signals, particularly that corresponding to Q^3 species, also occurs. The fwhm increases from 0.49 to 0.54 for Q^4 and from 0.50 to 1.24 for the Q^3 resonance. The $Q^4/(Q^4 + Q^3)$ ratio increases from 0.49 to 0.56, indicating that the treatment produced some condensation of the framework. Besides, there is a third minor broad peak at $\delta = -103.5$ ppm, probably due to a different Q^3 environment, that amounts ca. 5% of the total silicon. Further broadening of the two main resonances, together with a small upfield shift to −100.5 (Q^3) and −111.5 ppm (Q^4), occur when sample R3a is submitted to hydrothermal treatment (Figure 11, spectrum c). Nonetheless, the magnitude of the peak broadening is small and suggests that the silicate layers remain crystalline. The changes caused in the spectra by the hydrothermal treatment can be attributed, therefore, to a relaxation of the crystalline structure of the silicate layer due to the formation of pores. It is noteworthy that the lines in spectrum c seem to have a very broad base. Such broad bases do not allow the lines to be fitted to any combination of Gaussian and Lorentzian functions and suggest that there is an additional broad signal, ranging approximately from −98 to −120 ppm, that overlaps with the narrow resonances attributed to the crystalline silicate. This broad signal could be attributed to the thin amorphous silica phase observed by TEM in the outer part of the particles with mesoporous lamellar structure, shown in Figure 8b.

The spectra of sample R3c after removal of the intercalated surfactant, either via treatment with ozone (spectrum d) or calcination in air (spectrum e), show broad signals, suggesting that the crystalline structure is lost. However, both treatments produce notably different materials (the inset of Figure 11 shows enlarged spectra for better comparison). The spectrum of the ozone-treated sample can be deconvoluted into two broad Gaussian functions centered at −112 and −104 ppm, corresponding to Q^4 and Q^3 silicon nuclei, with a $Q^4/(Q^3 + Q^4)$ ratio close to 0.5. On the other hand, the spectrum of the sample calcined in air shows a much lower intensity in the low field region, while the line centered at −112 ppm increases. These results indicate that higher concentration of Q^4 species, and therefore a more condensed silicate framework, is produced when the surfactant is removed at higher temperature. Furthermore, this later treatment also leads to broader resonances, suggesting that treatment with ozone might preserve part of the atomic ordering of the inorganic framework.

Discussion

On the basis of the above findings, the formation of the mesoporous material from RUB-18 can be summarized in

(23) Wolf, I.; Gies, H.; Fyfe, C. *J. Phys. Chem.* **1999**, *103*, 5933.

Scheme 1. Model of the Formation of the Crystalline Mesoporous Layer Silicate by CTA^+ Surfactant Intercalation in Na−RUB-18, Followed by Hydrothermal Treatment (HT), and Zeolite Crystals Growth after Prolonged HT

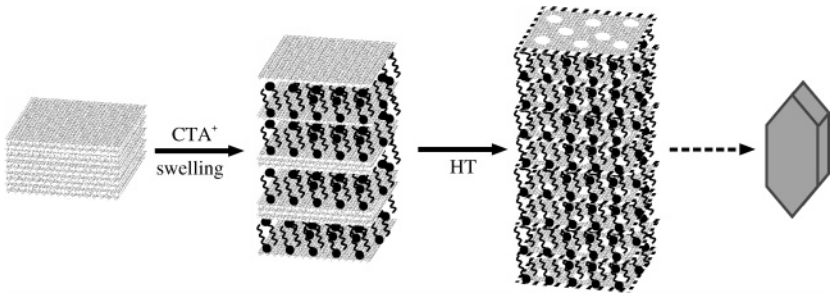

two stages that are depicted in Scheme 1. In a first stage, refluxing with the surfactant solution causes the swelling of the parent Na−RUB-18 silicate, according to XRD data that show the formation of a lamellar phase with a basal spacing of 2.78 nm. SEM, TEM/SAED, FTIR, and ^{29}Si MAS NMR studies indicate that the refluxing substantially altered neither the morphology nor the crystalline layer of RUB-18. The swelling is however accompanied by a small broadening of the ^{29}Si MAS NMR lines, which can be attributed to a certain deformation of the crystalline sheets produced by the intercalation of the surfactant molecules. Elemental analyses and FTIR spectra demonstrate that the surfactant is incorporated between the Na−RUB-18 layers by an ion exchange of the interlayer $Na(H_2O)_6^+$ cations, giving rise to the swelling of the host material. In the limited interlayer space of Na−RUB-18, the charge is arranged in a flat manner, and then it is feasible for the surfactant to form a lamellar phase.

In the second stage, the RUB-18 layer is transformed into a mesoporous phase during the hydrothermal treatment. TEM images show that these mesopores appear fairly ordered and oriented in a direction perpendicular to the silicate layer. Therefore, the pore length is very short. If pores were restricted to a single layer, an increase of the number of Q^3 species would be expected. However, the ^{29}Si MAS NMR results indicate that this is not the case. This suggests that a condensation of the defects (Si−OH/Si−O^-) to siloxane bridges occurs in the border of the mesowindows formed in neighboring layers. Therefore, the pore length extends across several layers. The creation of this mesostructure is also evidenced by the development of a low-angle reflection in the XRD pattern. From the calculated unit cell parameter of such mesostructure and the pore size determined by nitrogen sorption measurements after removal of the surfactant by calcination, pore wall values have been estimated to be as large as 4 nm. As a consequence of this, surface area values of the mesoporous materials do not exceed 250 m^2/g.

Although the exact mechanism of a possible solid-phase transformation remains unclear, a square mesostructure observed by TEM in some thin, inner areas may be the intermediate in the transformation of the parent crystalline silicate framework. The narrow framework vibration bands and ^{29}Si resonances observed for the hydrothermally treated samples strongly support that the silicate framework is highly crystalline. The small broadening of the signals observed in FTIR and ^{29}Si MAS NMR spectra may be related to the reorganization of the RUB-18 building units into a less long-range ordered silicate species, required otherwise to form the mesopores clearly visible in the TEM images. A very thin lamellar mesostructure is also observed by TEM in the outer part of the crystals that seems to be the result of a local dissolution and recrystallization of silicon species in the early stages of the phase transformation. This phase is probably amorphous and might be associated with the additional broad Q^3 and Q^4 resonances observed in the ^{29}Si MAS NMR spectrum of the hydrothermally treated sample. The occurrence of dissolution and recrystallization processes are also manifested by the growth of zeolite crystals after prolonged hydrothermal treatment. The formation of this silicalite-1 phase probably implies that extensive hydrotermal treatment also produces degradation of the surfactant species, generating smaller organic entities able to template the formation of the MFI structure.

Attempts to remove the surfactant by calcination in air at 450 °C resulted in the loss of crystallinity of the mesostructured layer material. Even the use of a lower temperature treatment with ozone to remove the surfactant has a marked effect on crystallinity. However, the material obtained by ozone treatment at 200 °C exhibits narrower ^{29}Si resonances, which suggests a higher degree of order of the silicate framework. Furthermore, FTIR spectroscopy shows that crystalline subunits of the parent silicate are present in this material. HRTEM/SAED studies also evidenced that some atomic fringes are present in the final mesoporous material when surfactant removal was performed at lower temperature with ozone.

Despite the loss of crystallinity produced by the thermal treatments used to remove the surfactant, TEM images and XRD patterns show that the mesostructure of the silicate layers is preserved. N_2 sorption measurements show that both surface area and pore volume of these samples are in agreement with those of a conventional MCM-41. In conclusion, the retention of the platelike morphology coupled to the ordered mesoporous structure formation leads to a very interesting mesoporous material with short pores perpendicular to the plate plane. This finding is of a particular interest since it implies a short path through the pores and suggests its possible application to the synthesis of mesoporous membranes.

Conclusions

A novel method to prepare a mesoporous material stable to calcination has been achieved through the reaction of the complex layered silicate precursor Na−RUB-18 with the cationic surfactant cetyltrimethylammonium chloride fol-

lowed by a hydrothermal treatment. As a result, the as-prepared mesoporous material shows crystal morphology and local atomic arrangement similar to that of the crystalline precursor silicate. TEM studies reveal flat and thin crystals with mesoporous channels in the direction perpendicular to the plate plane of the crystals. This methodology of synthesizing mesoporous materials from multilayered precursors opens up a field for further development on the search of mesoporous materials with highly ordered frameworks.

Acknowledgment. Financial support of Spanish Ministry of Education and Science (MEC), project MAT 2003-07769-C02-02, is acknowledged. R.G. wishes to acknowledge MEC for a "Juan de la Cierva" postdoctoral grant. We are grateful to Prof. O. Terasaki and Dr. T. Ohsuna for helpful discussion of the Na−RUB-18 TEM/SAED results. Finally I.D. acknowledges Prof. H. Gies for experimental details of the synthesis of Na−RUB-18.

CM052855M